9

Effects of Interaction of Electromagnetic Waves in Complex Particles

Ludmilla Kolokolova[1], Elena Petrova[2] and Hiroshi Kimura[3]
[1]*University of Maryland, College Park,*
[2]*Space Research Institute, Moscow,*
[3]*Center for Planetary Science, Kobe*
[1]*USA,*
[2]*Russia,*
[3]*Japan*

1. Introduction

The majority of natural materials (rocks, soil, wood, etc.) are inhomogeneous and have a complex structure. Very often they are conglomerates or aggregates, i.e. made of small grains stuck together. This is especially typical for planetary aerosols and all types of cosmic dust (interstellar, circumstellar, interplanetary, cometary, etc.). Cosmic dust, specifically, cometary will be the main test object for this paper. This is related to the fact that cosmic dust is usually studied through remote sensing, specifically through the study of electromagnetic waves it scatters and emits. Due to this, the field of light scattering by cosmic dust has always been at the frontier of the study of interaction of electromagnetic waves with non-spherical and inhomogeneous particles. It has inspired publication of the scholarly books by van de Hulst (1957), Schuerman (1980), Kokhanovsky (2001), Hovenier et al. (2004), Voshchinnikov (2004), Borghese et al. (2010), and Mishchenko et al. (2000, 2002, 2010) and numerous book chapters, e.g., Mukai (1989), Lien (1991), Gustafson (1999), Gustafson et al. (2001), Kolokolova et al. (2004a, b).

To consider the scattering of electromagnetic waves by an object of complex structure, we will determine this object as a configuration of discrete finite constituents. They will be called inclusions in the case of inhomogeneous particles, or monomers in the case when they are constituent particles of an aggregate. Their volume is large enough that we may ignore their atomic structure and characterize their material by a specified complex refractive index, $m=n+i\kappa$, whose real part is responsible for the refraction and imaginary part for the absorption of the light by the material. The surrounding medium is assumed to be homogeneous, linear, isotropic, and, in the case of aggregates, non-absorbing. Although we discuss some approximations, our consideration is based on the Maxwell equations fully describing the interaction of the electromagnetic radiation with the material. The non-linear optical effects, non-elastic scattering, quickly-changing illumination and morphology of the scattering object are beyond the scope of our study.

As mentioned above, our test example will be cosmic dust that typically can be presented as aggregates of submicron monomers. In the optical wavelengths they are good

representatives of inhomogeneous particles with inclusions of size comparable with the wavelength, more exactly of size parameter $x=2\pi a/\lambda > 1$ where a is the radius of the monomers and λ is the wavelength. The main light scattering characteristics that we use in our consideration are intensity (the first Stokes parameter, I) and linear polarization, P. The latter we describe as $P=Q/I$ where Q is the second Stokes parameter; $P>0$ when the scattering plane is perpendicular to the polarization plane and $P<0$ when the scattering plane coincides with the polarization plane. We ignore the third Stokes parameter U since in the vast majority of the observational data the third Stokes parameter is equal to zero. We mainly consider how electromagnetic scattering affects phase curves, i.e. dependences of I and P on the phase angle, α, i.e. the angle source-scatterer-observer. It is related to the scattering angle as 180°- α. The phase curves typical for cosmic dust are presented in Fig. 1.1. Their major features that we will discuss later are forward and back scattering enhancements in the intensity phase curve and negative polarization at small phase angles. In Section 5 we also briefly consider spectral dependence of the intensity and polarization and circular polarization defined as V/I where V is the fourth Stokes parameter. All the ideas considered below can be easily extended to the case of other complex particles or media with inhomogeneities characterized by $x>1$.

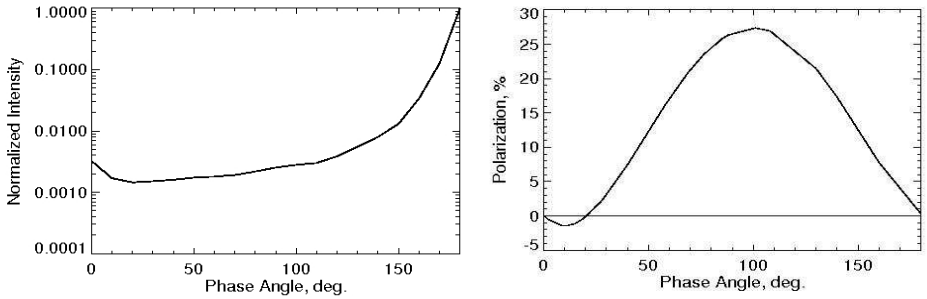

Fig. 1.1. Typical phase curves of intensity (left) and polarization (right) for cosmic dust. Intensity is normalized to the value at 180°. Notice forward and back scattering enhancements in the intensity curve and a negative polarization branch in the polarization curve at small phase angles.

In Sections 2-4 we consider main interactions between constituents of a complex particle and describe the conditions and consequences of these interactions. The focus of our consideration is how the electromagnetic interactions change as the constituents (e.g. monomers in aggregates) become more closely packed. In Section 5 we discuss the results of rigorous computer simulations of the electromagnetic interactions. The simulations are illustrated by the results of computer modeling of light scattering by aggregates. For the modeling, we use the T-matrix approach for clusters of spheres by Mackowski & Mishchenko (1996) that, being a rigorous solution of the Maxwell equations, allows us to account for all physical phenomena that occur at the light scattering by aggregates of small particles, including far-field and near-field effects, and diffuse and coherent scattering.

2. Electrostatic approximation: Effective medium theories

An extreme case of electromagnetic interaction between constituents of a complex particle occurs when this interaction can be considered in the electrostatic approximation. This consideration works when a complex particle can be represented as a matrix material that contains inclusions and both the size of the inclusions and distances between them are much smaller than the wavelength. This approach implies that the inhomogeneous particle is much larger than the inclusions and can be considered as a medium. Such a medium can be presented as homogeneous and characterized by some "effective" refractive index whose value can be found if refractive indexes of the matrix and inclusion materials are known. Such an approach to the complex particles (or media) is called mixing rules or effective medium theories. After the effective refractive index is found, it can be used to model the material of the particle whose size and shape correspond to the macroscopic particle and then consider scattering of radiation by such a macroscopic particle as if it is homogeneous. Numerous mixing rules have been developed for a variety of inclusion types (non-Rayleigh, non-spherical, layered, anisotropic, chiral) and their distribution within the medium including aligned inclusions and fractal structures (see, e.g., Bohren & Huffman, 1983; Sihvola, 1999; Choy, 1999; Chylek et al., 2000). However, still the most popular remain the simplest Maxwell Garnett (1904) and Bruggeman (1935) mixing rules. The Maxwell Garnett rule represents the medium as inclusions embedded into the matrix material and the result depends upon which material is chosen as the matrix. The Bruggeman rule was obtained for a conglomerate of particles made of materials with the refractive indexes of inclusions and matrix embedded into the material with the effective refractive index. This formula is symmetric with respect to the interchange of materials and can be easily generalized for the n-component medium.

As we mentioned above, the derivation of the mixing rules is based on an assumption that the external field is an electrostatic one, which requires the inclusions to be much smaller than the wavelength of electromagnetic wave. More exactly, the criterion of the validity of effective medium theories is $xRe(m)<<1$ (Chylek et al., 2000) where x is the size parameter of inclusions and $Re(m)$ is the real part of the refractive index for the matrix material. Comparison of effective medium theories with more rigorous calculations, e.g. those that use Discrete Dipole Approximation, DDA (Lumme & Rahola, 1994; Wolff et al., 1998; Voshchinnikov et al., 2007; Shen et al., 2008), and experiments (Kolokolova & Gustafson, 2001) show that even for $xRe(m) \sim 1$ effective medium theories provide reasonable results. The best accuracy can be obtained for cross sections and the worst for polarization, especially at phase angles smaller than 50° and larger than 120°.

There were a number of attempts to consider heterogeneous grains using effective-medium theories, particularly to treat cosmic aggregates as a mixture of constituent particles (inclusions) and voids (matrix material) (e.g. Greenberg & Hage, 1990; Mukai et al., 1992; Li & Greenberg, 1998b; Voshchinnikov et al., 2005, 2006). In the visual these aggregates with the monomer size parameter of $x > 1$ are, most likely, out of the range of the validity of the effective medium theories. However, for the thermal infrared, cosmic aggregates can be treated with the effective medium theories if they are sufficiently large; remember, that the macroscopic particle should be large enough to allow considering it as a medium.

If the distance between inclusions becomes larger than the wavelength, the electrostatic approximation should be replaced by the far-field light scattering (see Section 3). If the inclusions or monomers in aggregates become comparable or larger than the wavelength i.e.

the criterion $xRe(m)<1$ is violated, cooperative effects in electromagnetic interaction between the inhomogeneities become dominating. To account for them one needs to consider rigorously the interaction of electromagnetic waves that occurs in such complex objects counting on the near-field effects (Section 4).

3. Far-field light scattering

The fundamental solution of the Maxwell equations as a harmonic plane wave describes the energy transfer from one point to another. The plane electromagnetic wave propagates in the infinite nonabsorbing medium with no change in intensity and polarization state. The presence of a finite scattering object results in modification of the field of the incident wave; this modification is called the electromagnetic scattering.

If the scattering object (e.g., particle) is located from the observer at such a distance that the scattered field becomes a simple spherical wave with amplitude decreasing in inverse proportion to the distance to the scattering object, the equations describing the scattered field become much simpler. This is the so-called far-field approximation. There are several criteria of this approximation (e.g., Mishchenko et al., 2006, Ch. 3.2): $2\pi(R-a)/\lambda >>1$, $R>>a$, and $R>>\pi a^2/\lambda$, where R is the distance between the object and the observer and a is the radius of the object. The first relation means that the distance from any point inside the object to the observer must be much larger than the wavelength. Then, the field produced by any differential volume of the object (the so-called partial field) becomes an outgoing spherical wave. The second relation requires the observer to be at a distance from the object much larger than the object size. Then, the spherical partial waves coming to the observer propagate almost in the same direction. The third relation can be interpreted as a requirement that the observer is sufficiently far from the scatterer so that the constant-phase surfaces of the waves generated by differential volumes of the scattering object locally coincide in the observation point and form an outgoing spherical wave.

If the scattering object is an ensemble of particles, it is convenient to present the total scattered field as a vector superposition of the fields scattered by individual particles and, thus, to introduce the concept of multiple scattering. It is worth noting that at multiple scattering the mutual electromagnetic excitations occur simultaneously and are not temporally discrete and ordered events (Mishchenko et al., 2010). However, the concept of multiple scattering is a useful mathematical abstraction facilitating, in particular, the derivation of such important theories as the microphysical theories of radiative transfer and coherent backscattering (see below).

In some cases the scattering by a complex object can be considered in the far-field approximation that substantially simplifies the equations that describe the scattering. The conditions for this are the following: (1) the constituent scatterers of the complex object are far from each other to allow each constituent to be in the far-field zone of the others, and (2) the observer is located in the far fields of all of the constituent scatterers. Natural examples of such objects are atmospheric clouds and aerosols.

3.1 Diffuse light scattering

The properties of the light that is scattered by an ensemble of scatterers (e.g., small particles) only once are fully determined by the properties of the constituents. If the particles are much smaller than the wavelength, they scatter light in the Rayleigh regime and produce

symmetric photometric phase function with the minimum at 90° and also symmetric, bell-shaped, polarization phase function with the maximum at 90°. For larger particles, the phase curves demonstrate a resonant structure with several, or even numerous, minima and maxima in both intensity and polarization depending on the size parameter of particles and the refractive index. Nowadays, the single scattering properties can be reliably calculated for particles of various types (e.g., Mishchenko et al., 2002).

If a complex object can be presented as a cluster of sparsely distributed particles, i.e. the far-field requirements are satisfied, the intensity of light scattered by the object is proportional to the number of constituents, N. While the number N and the packing density are increasing, the effects of mutual shadowing, multiple scattering, interference, and the interaction in the near field may destroy this dependence.

The evolution of the scattering characteristics of a cluster of separated particles with increasing number of the constituent partciels can be illustrated with the results of model calculations preformed with the T-matrix method for randomly oriented clusters of spheres (Mackowski & Mishchenko, 1996). We consider a restricted spherical volume and randomly fill it with small non-intersecting identical spheres (in the same manner as Mishchenko, 2008; Mishchenko et al., 2009a, b; Petrova & Tishkovets, 2011; see example in Fig.3.1). In Fig. 3.1 we show the absolute values of intensity and the degree of linear polarization calculated for a single small nonabsorbing spherical particle and the volume containing different number of such particles. There we define the intensity as $F^{11}Q_{sca}X_v$, where F^{11} is the first element of the scattering matrix normalized in such a way that this quantity integrated over all phase angles is equal to unity, Q_{sca} is the scattering efficiency of the cluster, and X_v is the size parameter of the cluster calculated from the volume of the constituents as $x_1N^{1/3}$.

When the number of particles in the cluster grows, the amplitude of the bell-shaped branches of polarization decreases, and the curves of intensity in the phase interval from 20° to 150° become flatter. If the phase curves for individual particles contained substantial interference features typical for relatively large spheres (larger than the particles considered in the example in Fig. 3.1), these features would be continuously smoothed with increasing packing density (see, e.g., Mishchenko, 2008). Such a smoothing can be interpreted as a result of the increasing contribution of multiple scattering, when many scattering events force light to "forget" the initial direction and to contribute equally to all exit directions. This also causes the depolarization effect, i.e. the light multiply scattered by an ensemble of particles is characterized by smaller values of polarization than the polarization of the light scattered by an individual particle of the ensemble. This happens since the position of the scattering plane changes at each consequent scattering, thus changing the polarization plane of the scattered light. Multiple changes that resulted from multiple scattering by randomly distributed particles randomize the polarization plane and, thus, lower the polarization of the resultant light. It is remarkable that diffuse multiple scattering is unable to change the state of polarization. As a result of this, the polarization always changes its sign at the same phase angle as for an individual particle no matter how many particles are in the cluster (Fig 3.1).

Since the behavior of the diffuse multiple scattering in the sparse media is rather well investigated in the framework of the radiative transfer theory, here we only recall the main properties of the scattered electromagnetic radiation. It increases, when either the particle size, or the number of particles in the medium, or the real part of the refractive index, or the packing density grow. If the imaginary part of the refractive index increases, the contribution of the radiation scattered twice predominates. The latter is partially polarized

and can strongly depend on phase angle. For densely packed clusters or media, a study of the scattering based on the diffuse scattering is not relevant as it lacks consideration of such effects as shadowing and near-field interaction (see Section 4).

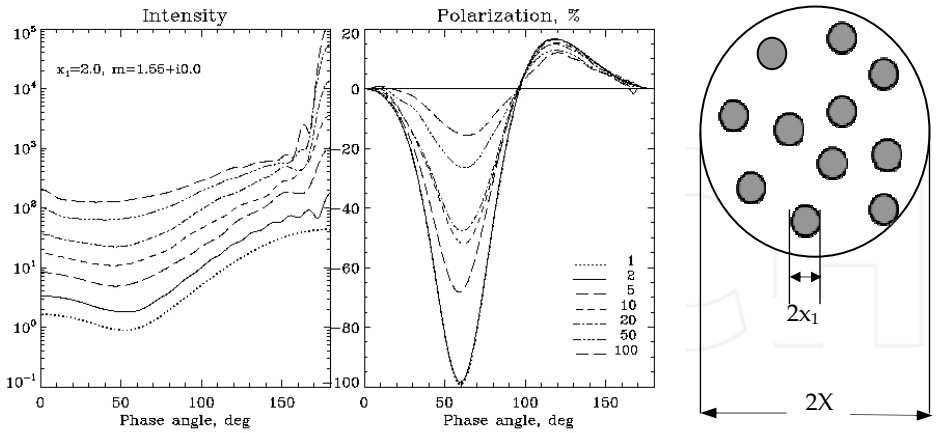

Fig. 3.1. The intensity and polarization of light scattered by a single spherical particle (dotted curve) and clusters of such particles contained in the volume of the size parameter X=20. The values of the size parameter x_1 and the refractive index m of the constituent particles and the number of particles in the volume are listed in the figure. The packing density of the cluster (defined as $\rho = N x_1^3 / X^3$) grows from 0.1% to 10% (for N=1 and 100, respectively). An example of the cluster is shown on the right.

Numerous computations have shown that the light-scattering characteristics of aggregates substantially differ from those of a cluster of separated monomers and change if the structure and porosity of the aggregates change (West, 1991; Lumme & Rahola, 1994; Kimura, 2001; Kimura et al., 2003, 2006; Mann et al., 2004; Petrova et al., 2004; Tishkovets et al., 2004; Mishchenko & Liu, 2007; Mishchenko et al., 2007; 2009a; 2009b; Zubko et al., 2008; Okada & Kokhanovsky, 2009; and references therein). These changes cannot result from the diffuse multiple scattering between the aggregate monomers, which can only suppress the resonant features typical for the phase function of constituents and depolarize the scattered light. The specific shape of the phase curves shown in Fig. 1.1 is caused by more complex cooperative effects.

A striking feature in the intensity phase curve in Fig 1.1 is a strong increase of the intensity as the phase angles become larger than 160°. Development of such an increase with increasing number of the particles in the volume is evident in the plots shown in the left panel of Fig. 3.1. This strong forward scattering enhancement is caused by constructive interference of light scattered by the particles in the exact forward direction. In this direction, the waves scattered once by all the particles are of the same phase (if the particles are identical) irrespective of the particle positions (see Bohren &Huffman, 1983; Section 3.3). The oscillating behavior of the intensity curves in the forward scattering domain also points to the interference nature of this feature. In the absence of multiple scattering, this interference would result in an increase of intensity by a factor of $N(N-1)$ as compared to the scattering by a single particle or by a factor of N^2, if the non-coherent single scattered components are taken into account. Such an increase

is really observed, when the packing density is small. However its development slows down with increasing packing density and practically stops, when the packing density exceeds approximately 15%. Such a behavior results from the fact that the incident light exciting a particle gets attenuated by its neighbors. This effect finally leads to the exponential extinction of light considered in the radiative transfer theory. The polarization caused by the single scattering interference in the forward scattering region is the same as that for the constituents, if they are identical.

One more interesting feature starts to develop in the intensity phase curve when the number of particles in the volume grows. This is the enhancement toward zero phase angle, which becomes noticeable at N=50 at phase angles smaller than 15°. It is accompanied by a change in the polarization state at small phase angles. These features are a typical manifestation of the coherent-backscattering (or weak-localization) effect, which is considered in the next section.

3.2 Coherent backscattering effect

The enhancement of intensity that started to emerge in the backscattering domain (Fig. 3.1), when the packing density approached 5%, is a frequent feature of the phase curves of many scattering objects observed in laboratory (particulate samples) or in nature (regolith surfaces). This is the so-called brightness opposition effect. Explanation of its origin is illustrated in Fig. 3.2a (see Mishchenko et al., 2006 and references therein). The conjugate waves scattered along the same sequence of particles in the medium but in opposite directions interfere, and the result depends on the respective phase differences. For any observational direction far from the exact backscattering, the average effect of interference is negligible, since the particle positions are random. However, at exactly the backscattering direction, the phase difference is always zero and, consequently, the interference is always constructive, which causes the intensity enhancement to the opposition. This effect is called coherent backscattering.

Interference in the backscattering direction may manifest itself in one more effect: it may lead to appearance of a branch of negative polarization at small phase angles (the so-called polarization opposition effect). This effect is schematically explained in Fig. 3.2b (also see Shkuratov, 1989; Muinonen, 1990; Shkuratov et al., 1994; Mishchenko, 2008). Particles 1-4 are in the plane perpendicular to the direction of the incident nonpolarized light. The particles 1 and 2 are in the scattering plane, while particles 3 and 4 are in the perpendicular plane. Let us assume that the particles are small relatively to the wavelength. Then they scatter light in the Rayleigh regime; the radiation scattered by such a Rayleigh particle is positively polarized for all phase angles. For the light scattered by the pair of particles 1-2, the resultant polarization keeps the polarization plane of the single scattering, i.e. it stays positive. However, the light scattering by the pair 3-4 occurs in the plane perpendicular to the resultant scattering plane; this makes the light scattered by this pair polarized in the scattering plane, i.e. negatively. The phase difference between the waves passing through particles 3 and 4 in opposite directions is always zero, while for particles 1 and 2 such phase difference is zero only at exactly the backscattering direction and quickly changes with changing the phase angle. Consequently, the conditions for negative polarization of the scattered light are on average more favorable in a wider range of phase angles than those for positive polarization. This forms a branch of negative polarization with the minimum at a phase angle whose value is comparable with the width of the brightness peak of coherent backscattering. Since only definite configurations of particles contribute to this effect, polarization opposition effect is less strong than the opposition effect in intensity.

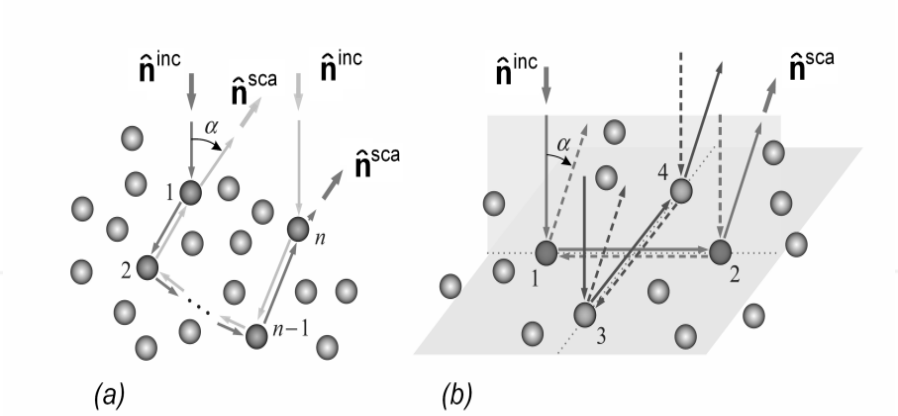

Fig. 3.2. Schematic explanation of the coherent backscattering effect (from Mishchenko, 2009a, b).

An example of such a behavior is shown in Fig. 3.3. It is seen that the formation of the intensity enhancement at small phase angles is accompanied by development of a negative polarization branch as the number of particles in the ensemble grows. Notice that the effect results from the fact that the polarization of the single-scattered light is positive. If the polarization of the single scattered light is negative, the interference results in positive polarization. If the polarization of singly scattered light changes its sign at a specific scattering angle, the interference leads to a complex angular dependence of polarization for the ensemble of scatterers as seen in Fig. 3.1.

In the interference presentation of the brightness and polarization opposition effects it was clearly assumed that the scatterers are in the far-field zones of each other, since some phase and polarization are attributed to the wave scattered by one particle and exiting the other one. However, recently it has been demonstrated that the conclusion on the interference nature of the opposition effects remains also valid for more closely packed media. In Fig. 3.4 we present some results obtained by Mishchenko et al. (2009a, b). They examined the influence of the packing density on the opposition phenomena in order to determine the range of applicability of the low-packing density concept of the coherent backscattering theory to densely packed media. As in the previous example, the ensemble of varying packing density was enclosed in a spherical volume of size parameter X (shown on the right of Fig. 3.4). When the number of particles in the volume of X=40 grows (N=500 corresponds to the packing density ρ=6.25%), the opposition peak grows, and the branch of negative polarization becomes deeper (Fig. 3.4 a-b). At the same time, the angular width of the opposition peak (determined as the angular position of the point, where the curve changes its slope) and the angular position of the polarization minimum are almost the same and remain constant with increasing number of particles. However, as the packing density grows (in Fig 3.4c this was achieved by decreasing the volume X) the shape of the negative branch transforms. To some value of the packing density, it is asymmetric, and its minimum is shifted to opposition as predicted by the theory of coherent backscattering (Mishchenko et al., 2006 and references therein). When the packing density grows up to substantial values (Fig. 3.4c, N= 300 that correspond to ρ = 30%), the effects related to the interaction of

particles in the near field become noticeable. They manifest themselves in the transformation of the shape of the negative branch and its widening, which we discuss in Section 4.

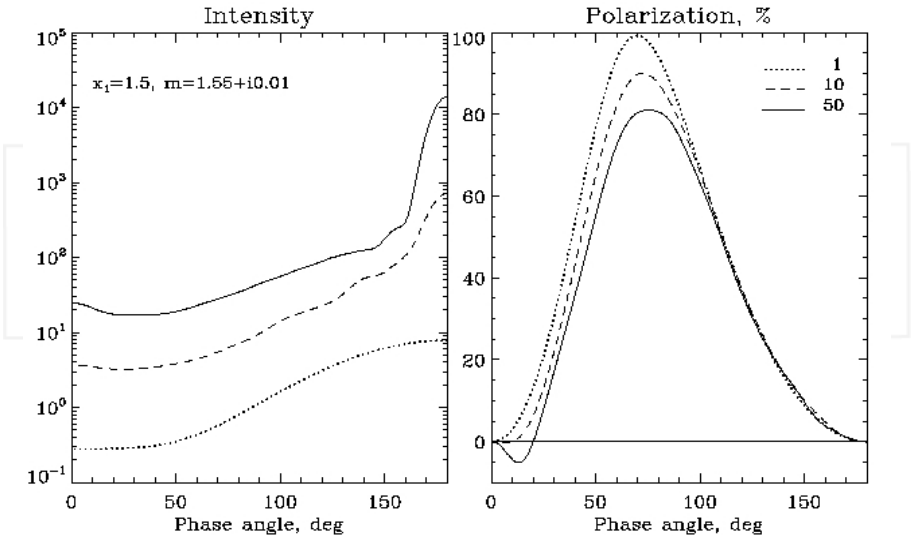

Fig. 3.3. Same as Fig. 3.1, but X=15, x_1=1.5, and m=1.55+i0.01. The numbers of particles in the volume are listed in the right top corner of the polarization plot.

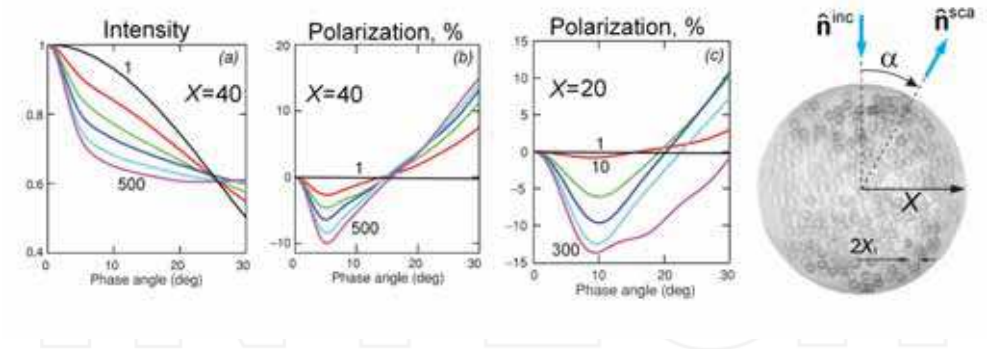

Fig. 3.4 The influence of the coherent backscattering on the intensity (normalized to the value at zero phase angle) and polarization of light scattered by ensembles of nonabsorbing spherical monomers of x_1=2 and m=1.32. Note that such individual monomers have polarization equal to zero in the backscattering domain and positive for the other phase angles. The size parameter of the volume X and the smallest and largest numbers of particles are shown in the plots. The geometry of the scattering ensemble is shown on the right. Adapted from Mischchenko et al. (2009b).

3.2.1 Some experimental facts

The above described opposition phenomena - a nonlinear enhancement of brightness to opposition and a negative branch of linear polarization of the scattered light – have been observed for cosmic dust in a variety of environments (debris disks, comets, Saturn's rings, asteroids and satellites of planets) as well as for laboratory particulate samples. Numerous experimental studies showed that the characteristics of these effects and their phase profiles are undoubtedly connected with absorption and microphysical structure of the scattering objects. In particular, it was found that a very sharp narrow brightness peak and an asymmetric branch of negative polarization with the minimum close to zero phase angle (less than 2°) are typical of bright and porous objects (see, e.g., the review by Rosenbush et al., 2002). These strongly expressed manifestations of the coherent backscattering mechanism appear due to a rather large free path of light in such a sparse particulate medium as regolith. Since the width of the coherent peak in intensity is inversely proportional to the free path, for extremely sparse media like atmospheric clouds this peak should be very narrow and cannot be observed. This peak also cannot be observed for the media that have a small restricted volume like small aggregates, especially if they are absorbing (e.g., Etemad et al., 1987). The absence of very sharp opposition features in aggregates and other individual particles of complex structure was confirmed by both observations of the cosmic dust and laboratory measurements (e.g., Levasseur-Regourd & Hadamcik, 2003; Shkuratov et al., 2004). This effect is also seen in Figs. 3.3-3.4 when the number of monomers in aggregates is small. These particles demonstrate a moderate increase of brightness to opposition and the branch of negative polarization with a shape close to symmetric.

Astronomical observations also revealed that dark or densely packed media demonstrate wider, if any, peaks of brightness near opposition and more symmetric branches of negative polarization (e.g., Shkuratov et al., 2002; Belskaya et al., 2005). This contradicts to the theory of coherent backscattering, which predicts that the opposition effects in brightness and polarization have the same cause and should appear simultaneously. Moreover, since only certain particle configurations contribute to polarization opposition effect, it might be less pronounced than brightness opposition effect. The shadow hiding, which is usually invoked to explain the widening of the opposition brightness peaks in dark surfaces (Lumme & Bowell, 1981), cannot induce such a significant negative polarization of the scattered light (e.g., Shkuratov & Grynko, 2005). Accurate consideration of the electromagnetic field in the particle vicinity, accounting for the presence of neighbor particles in the densely packed scattering clusters allows revealing one more scattering effect – the influence of the near field, which is considered in the next section.

4. Near-field effects

In the case of compact aggregates/media the electromagnetic interaction becomes even more complex, because the electromagnetic field in the close vicinity of the scattering particle is inhomogeneous due to the lag of the wave within the particle with respect to the incident wave. This effect is mostly expressed if the scatterer is comparable in size to the wavelength. Direct calculations using the Lorentz–Mie theory for spherical particles show that the constant phase surface of the total field is funnel shaped in the particle vicinity (Fig. 4.1a). Consequently, the field inhomogeneity near the particle causes a rotation of the total field vector relatively to the incident field vector. This results in the formation of a Z-

component of the total field that lies in the scattering plane and, consequently, reduces the scattered intensity in the back and forward scattering regions and increases the negative polarization (Tishkovets, 1998; Tishkovets et al., 1999; 2004a, b; Petrova et al., 2007).

To illustrate the influence of the field inhomogeneity in the vicinity of a particle, let us consider Rayleigh test particles located on a constant phase surface near a larger particle in its inhomogeneous zone (Fig. 4.1b). First, assume that the incident field is polarized in the scattering plane (as shown in Fig. 4.1a). If the test particles were far from each other and from other particles, i.e., in the homogeneous field, their dipole moments would be parallel to the x_0 axis. In this case, the intensity of the light scattered by all four test particles-dipoles would concentrate in the direction $\alpha = 0°$ and 180° and would be zero in the direction $\alpha = 90°$. If the test particles are, however, in the inhomogeneous zone near a wavelength-sized particle, the dipole moments induced in particles *1* and *3* have a nonzero component in the direction of wave propagation, i.e., along the z_0 axis. This results in decreasing intensity of the scattered light in the direction $\alpha = 0°$ and 180°, whereas the intensity in the direction $\alpha = 90°$ becomes nonzero. In both cases, the scattered wave is polarized the same way as the incident one, i.e. in the scattering plane (negatively). Now assume that the incident wave is polarized perpendicular to the scattering plane. Then particles *1* and *3* produce the radiation that is polarized perpendicular to the scattering plane and does not depend on phase angle. The radiation scattered by particles *2* and *4* has a component parallel to the z_0 axis (i.e., polarized in the scattering plane) that depends on α. As a result, the intensity again decreases in the directions $\alpha = 0°$ and 180° and increases in side directions, and polarization gets a negative component. So, at any polarization of the incident wave, the field inhomogeneity in the vicinity of the scattering particle induces a rotation of the field vector and leads to appearance of Z-component of the total field, which affects the angular distribution of the scattered intensity and causes negative polarization (for more details, see Tishkovets, 1998; Tishkovets et al., 1999; 2004a, b; Petrova et al., 2007).

One more type of interaction of particles in the near field is the mutual shielding of particles (Tishkovets, 2008; Petrova et al., 2009). The scheme with the test dipoles (Fig. 4.1b) helps to estimate qualitatively the result of the shielding. For the sake of simplicity, let us assume that at a given polarization of the incident radiation, the dipole moment of particle *1* is oriented exactly opposite to the k_{sc} vector. In this case, particle *1* does not radiate in the k_{sc} direction. It does not matter whether we take the shielding into account or not. When the incident radiation is polarized in the y_0z_0 plane, in the case of ignoring the shielding, particle *1* would radiate like particle *3* or like all the particles in the homogeneous field. However, when the large particle shields particle *1*, the latter does not radiate in the α direction, i.e., its positive polarization does not contribute to the scattered light. Thus, the shielding diminishes the positively polarized scattered radiation and diminishes the intensity in the α direction. However, in the backscattering direction, dipole *1* contributes to the scattered radiation, which induces an increase in the intensity with respect to that in the α direction. Contrary to the field inhomogeneity in the near zone, which is most noticeable for the wavelength-sized particles, the mutual shielding effect is independent of the size of the particles located in the near field.

Under the above described conditions the wave coming from one particle to another is not spherical, and the single-scattering characteristics of individual monomers, such as their phase matrix, are not applicable. In other words, in densely packed systems the scatterers become highly dependent. The influence of the interaction in the near field on intensity and

polarization of the scattered light can be easily demonstrated by the models, where the near-field contribution is ignored in the calculations of the light-scattering characteristics. The example presented in Fig. 4.2 clearly shows that the interaction in the near field substantially diminishes the backscattering peak in intensity induced by the coherent backscattering effect and changes the shape of the negative polarization branch.

Contrary to the coherent backscattering mechanism, the near-field effects work in a wide angular range. In the backscattering domain they distort the manifestations of the coherent backscattering. Their influence on polarization is rather complex and significantly depends on the size parameter of monomers, their packing density, and the refractive index. For example, with increasing packing density (i.e., when the near-field effects manifest themselves more clearly), the negative branch becomes deeper and wider if the aggregate is composed of larger monomers, while it may become shallower for smaller constituents. The modeling experiments with particles of different properties show that the most permanent and noticeable manifestation of the near-field effects in polarization is the shift of the polarization minimum out of opposition (Petrova et al., 2007; 2009). In other words, while the coherent backscattering mechanism forms the negative branch with the minimum near zero phase angle, the interaction in the near field causes the shift of the polarization minimum to larger phase angles and makes the negative polarization branch more symmetric.

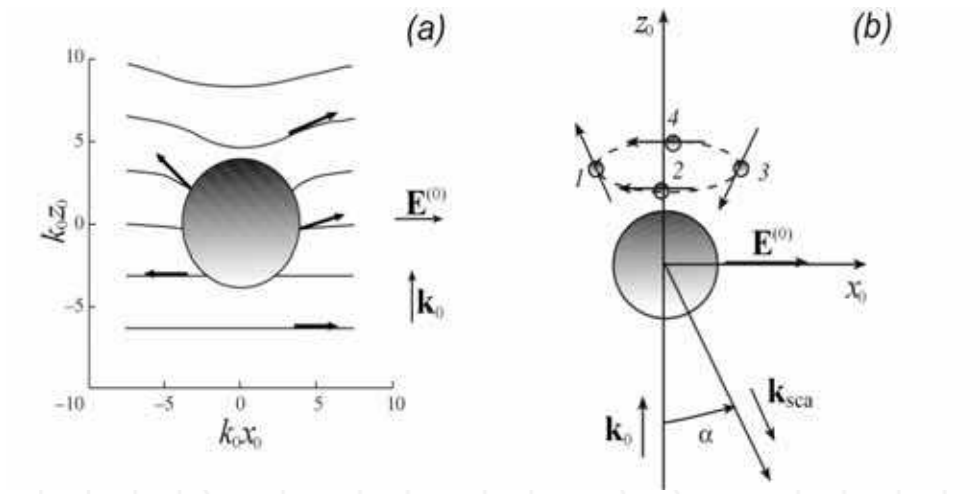

Fig. 4.1. (a) The scheme shows the constant phase surfaces and directions of electric field vectors (sum of the incident and scattered waves) in the close vicinity of a particle with x=4.0 and m = 1.32 + i0.05. The incident wave propagates along the wave vector $\mathbf{k}_0$ and is polarized in the x_0z_0 plane. Adapted from Tishkovets et al. (2004a). (b) The scheme for the scattering of inhomogeneous waves by the Rayleigh test particles 1 - 4. Particles *1* and *3* are in the x_0z_0 plane, while particles *2* and *4* are in the y_0z_0 plane. The incident wave propagates along the z_0 axis and is polarized in the x_0z_0 plane. The scattered wave propagates to the direction of the phase angle α. The vectors at the Rayleigh particles show the directions of the induced dipole moments. Adapted from Petrova et al. (2009).

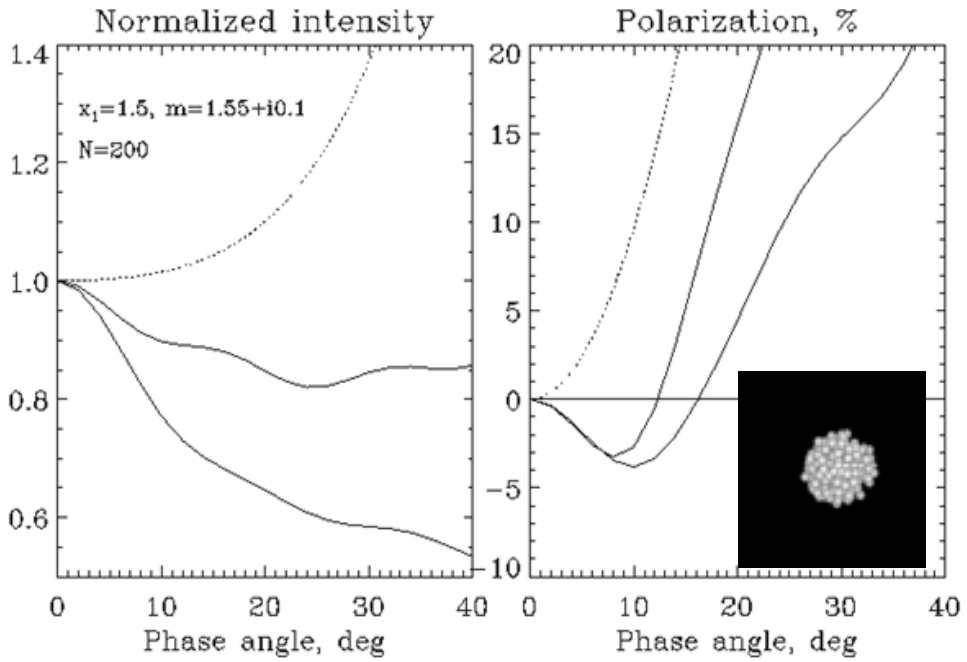

Fig. 4.2. The influence of the interaction in the near field on the intensity (normalized to the value at zero phase angle) and polarization in the backscattering domain for the compact cluster shown in the insert. Thick and thin curves present the models calculated with and without the near-field effects respectively. Dashed curves show intensity and polarization for the individual monomer. The parameters x_1, m, and N are shown in the figure. The data for the figures were kindly provided by V.P. Tishkovets.

Due to their nature, the manifestations of the near-field effects can be more easily observed in absorbing aggregates when the packing density exceeds 10-15%. One of such examples is shown in Figs. 4.3 for the whole range of phase angles and separately for the backscattering domain. For rather small number of monomers, the conditions for diffuse scattering and coherent backscattering are applied. With increasing number of monomers, the forward-scattering peak develops, the intensity profile becomes flatter, and the polarization maximum gets depressed. Then the opposition peak in intensity grows, and the negative branch of polarization appears. However, the opposition features do not develop as quickly as in nonabsorbing aggregates (compare Fig. 3.4), because the free paths become somewhat shorter when absorbing monomers are added into the volume. Partly due to this effect, partly due to the interaction in the near field - which becomes more important with increasing packing density - the polarization minimum moves out of opposition. Further increase of the packing density makes the near-field effects even more decisive. We see that the opposition peak stops to grow, while the negative branch continues to develop; it becomes wider and deeper (the curves for N=200).

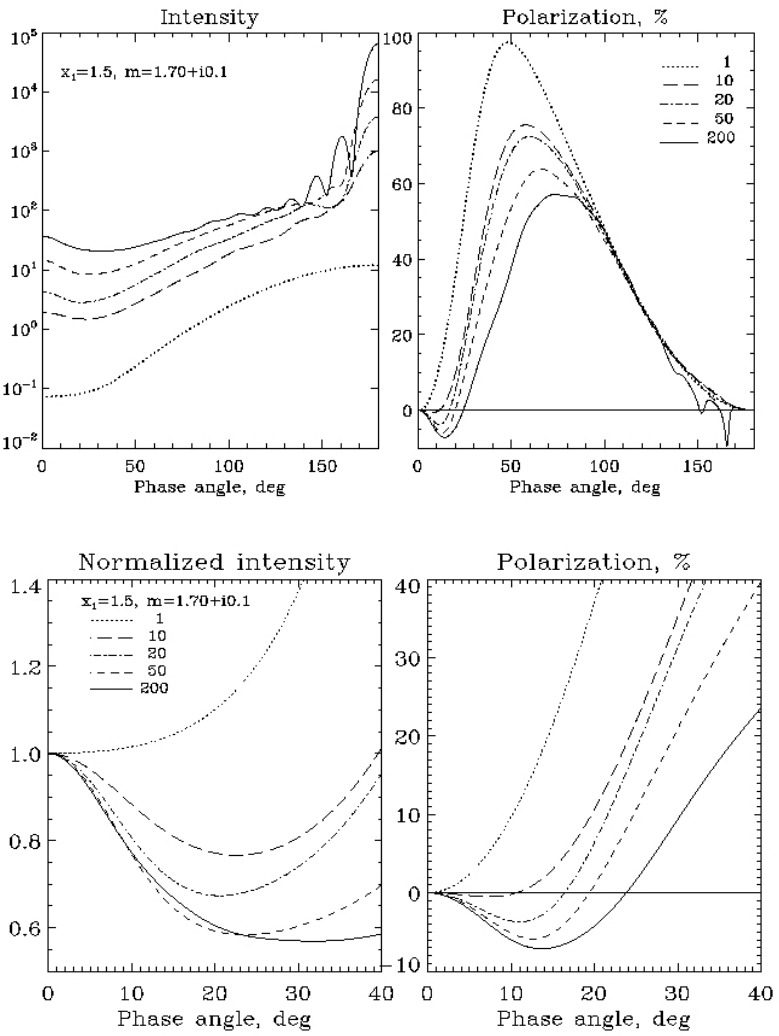

Fig. 4.3. Top panel: same as Fig. 3.1-3.3, but for the parameters listed in the plot. The packing density varied from 0.1% to 20% (*N* changes from 1 to 200, respectively). Bottom panel: larger scale for the backscattering domain; the intensity is normalized to the value at zero phase angle.

5. Modeling of light scattering by aggregates

In this section we explore how the considered above phenomena associated with electromagnetic interaction between constituents in a complex medium affect the angular and spectral dependence of intensity and linear polarization of the scattered radiation. We show how these results can be applied to the study of cosmic dust and other types of complex particles. We also briefly consider how the cooperative effects affect circular polarization of aggregates that contain optically active materials, e.g. complex organics of biological origin.

To model electromagnetic scattering by complex dispersed systems, several methods are now available. They are based on the numerically exact solutions of the Maxwell equations. One of them, the so-called superposition T-matrix method (Mishchenko et al., 2002; Mackowski & Mishchenko, 1996), was used to obtain the intensity and linear polarization of clusters of particles discussed above. Since these computations are time and resource consuming, they cannot be presently fulfilled for very large clusters/layers of particles, such as regolith. Nevertheless, they allow us to obtain the scattering characteristics of aggregates of a restricted number of monomers that are typical for cosmic dust, and to study the dependence of the light-scattering characteristics on the size of monomers, their packing density and refractive index.

5.1 Dependence of light scattering characteristics on the physical properties of aggregates

Exploring the light scattering characteristics of aggregates, we continue to focus on the dependence of intensity and linear polarization on phase angle, i.e. photometric and polarimetric phase curves. Our goal is to find out how the phase curves depend on such characteristics of aggregates as the size and composition of the monomers, their number and arrangement in the aggregate. In the previous sections we were mainly interested in the models of complex objects that allowed us to better see specific physical phenomena such as coherent backscattering or near-field effects. This section is directed to provide a basis for the interpretation of experimental data, specifically the observations of cosmic dust. This is why in this section we use more realistic models of natural aggregates, namely the aggregates grown under ballistic process (Meakin et al. 1984). There are commonly used two types of such aggregates: Ballistic Particle-Cluster Aggregate (BPCA) that grows at collision of individual monomers with the aggregate and Ballistic Cluster-Cluster Aggregate (BCCA) that grows at collision of clusters of monomers. Examples of such aggregates are shown in Fig. 5.1. Notice that BPCAs are usually more compact than BCCAs. The packing density of ballistic aggregates is defined as the ratio of the volume taken by their monomers to the total volume of the aggregate which is the volume of a sphere of the characteristic radius A calculated as $A^2 = 5/3 \sum_{i,j=1,\ldots N} (r_i - r_j)^2/(2N^2)$ (Kozasa et al., 1992) where r_i is location of the center of the i^{th} monomer and the total number of the monomers is N. Packing density depends on the number of monomers; as this number increases, it decreases significantly for BCCAs and slightly for BPCAs (Kolokolova et al., 2007).

The results of the modeling of the light scattering characteristics of BCCA and BPCA at some refractive indexes and monomer size are shown in Figs. 5.2 -5.3; for more results see LISA database at https://www.cps-jp.org/~lisa/. There instead of intensity I we use albedo, a characteristic that is usually used in astronomical observations to describe the reflectivity of an object. In the case of aggregates, albedo is defined as $(I/I_0)*(\pi/G)$ where I_0 is the intensity of the incident light and G is the aggregate geometric cross section (Hanner et al., 1981; Kimura et al., 2003). We show spectral dependence of albedo and polarization in two filters: 450 nm (blue filter) and 600 nm (red filter). Following astronomical definitions, if albedo or polarization have larger values in the red filter we say that they have a red color and if the values are larger in the blue filter we say that they have a blue color.

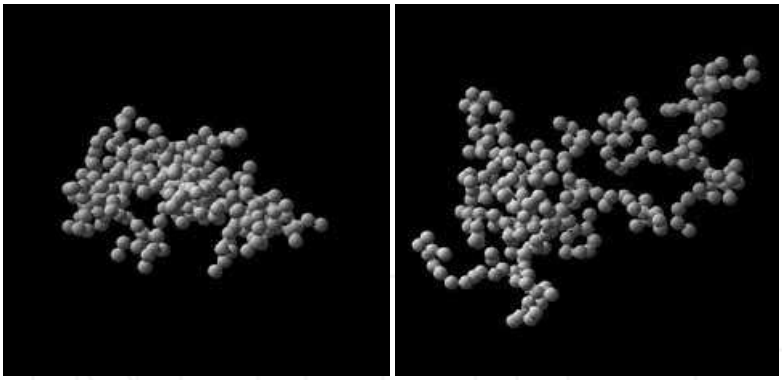

Fig. 5.1. Samples of BPCA (left) and BCCA (right) aggregates. These aggregates were used in Kimura et al. (2003, 2006) computations to model light-scattering characteristics of cometary dust.

First, notice in Fig. 5.2-5.3 the features of the modeled phase curves described in the previous sections, namely: (1) strong forward scattering resulted from the interference of the light single-scattered by individual monomers; (2) rather low values of the maximum polarization that manifests depolarizing effects of the diffuse scattering and influence of the near-field effects; (3) some, although small, backscattering enhancement; and (4) rather small but symmetric branch of negative polarization at small phase angles. The last two features indicate a serious influence of the near-field effects. This is not surprising as the monomers in aggregates touch each other, i.e. they do are located in the inhomogeneous field produced by their neighbors. As it was shown in Section 4, the near-field effects affect the shape of the intensity curve and result in a more pronounced and symmetric negative polarization branch and in diminished values of the positive polarization.

The figures also show a difference between the plots obtained for aggregates of different physical properties. The most influential parameter seems to be the monomer size whose variations change the shape of the polarization phase curve and the dependence of the albedo on the wavelength. The real part of the refractive index mostly affects the maximum polarization. The imaginary part of the refractive index affects the spectral dependence of photometric phase curve and the values of albedo but does not much affect polarization. Notice also that the more compact BPCAs depolarize the light more strongly than the more porous BCCAs, although their other characteristics are rather similar.

Although the curves in Figs 5.2-5.3 resemble the typical observational curves shown in Fig.1.1, they have some characteristics that are not typical for cometary dust. Observational facts summarized in Kolokolova et al. (2004a, b) indicate that comets usually have red photometric and polarimetric colors, i.e. their albedo and polarization have larger values at longer wavelengths. Unlike the observational data, the results of the modeling shown in Figs. 5.2-5.3 always demonstrate predominantly blue photometric color. In the case of the monomers of radius 120 nm and the refractive index equal to *1.4+i0.01*, the results of the modeling also demonstrate blue polarimetric color for some phase angles. Also, in the majority of plots, the value of albedo at zero phase angle is higher than the one observed, which is equal to 3 - 5% (Hanner, 2003).

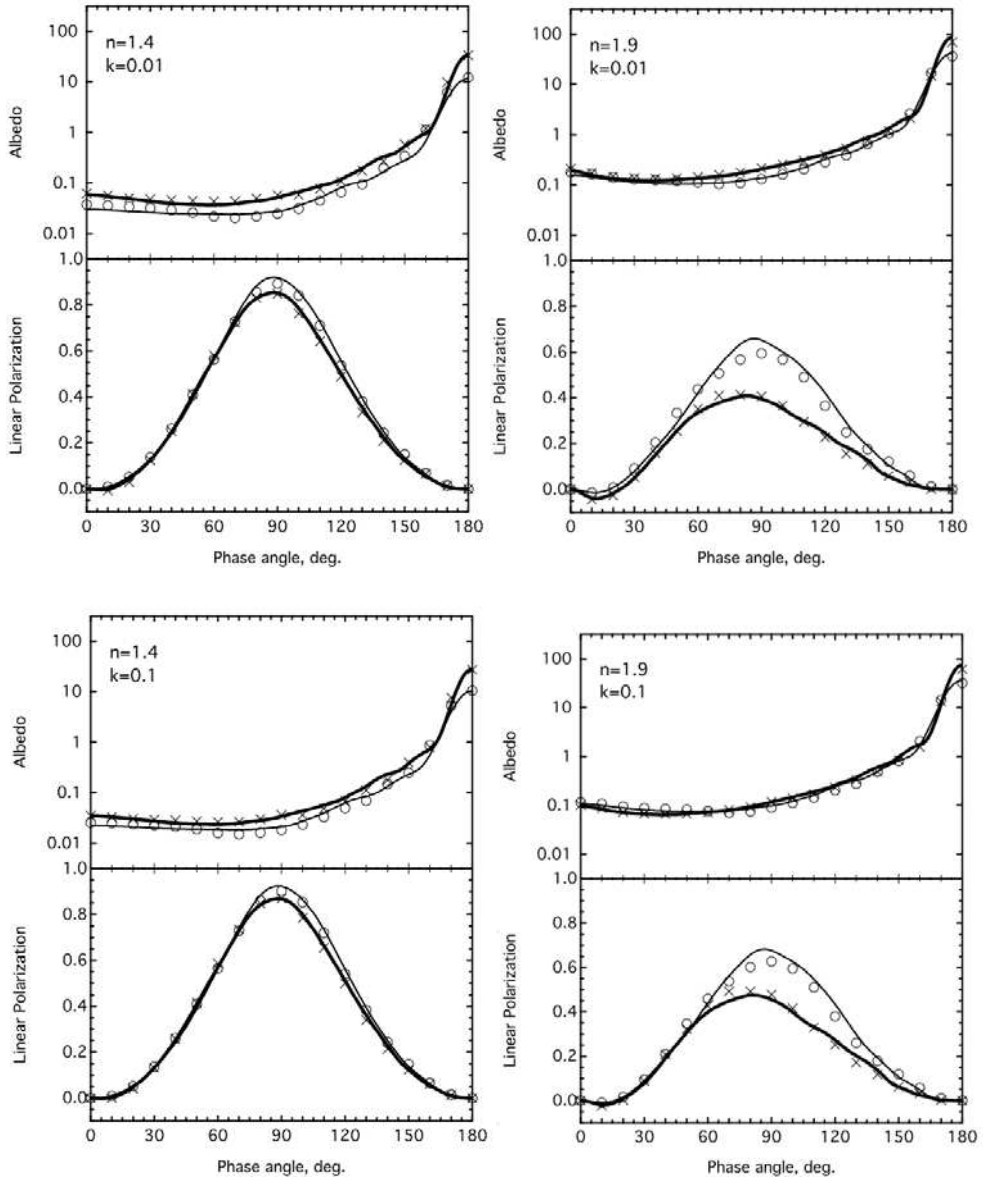

Fig. 5.2. Albedo (in %) and polarization as functions of phase angle for aggregates of monomer radius equal to 90 nm. Real part of the refractive index, *n*, and imaginary part of the refractive index, κ, are shown in the top left corner of each figure. Results for the wavelength 450 nm are shown by thick line (BCCA) and crosses (BPCA) and for 600 by thin line (BCCA) and circles (BPCA). All aggregates consisted of 128 monomers.

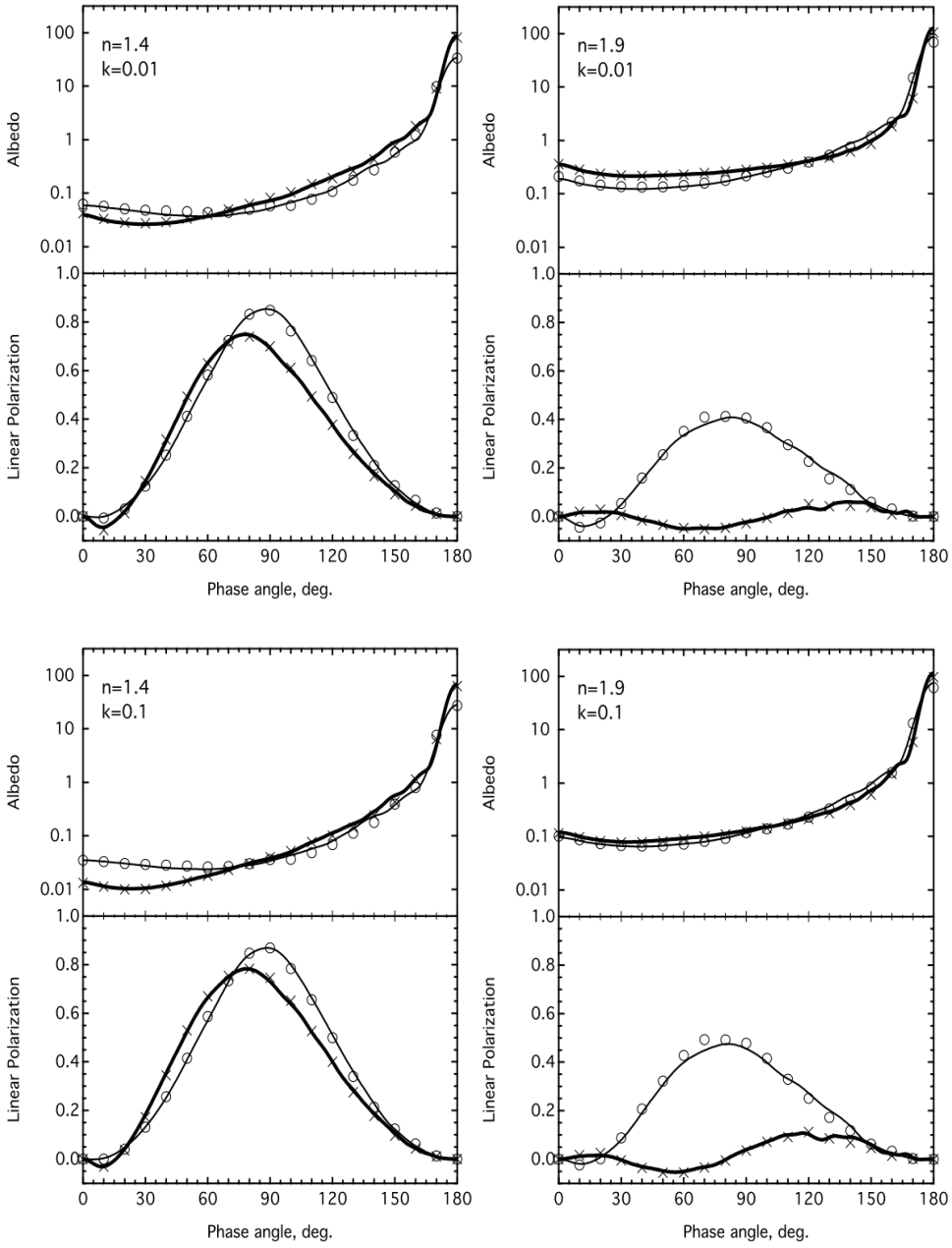

Fig. 5.3. The same as Fig. 5.2 but for monomers of radius 120 nm.

Our computations, summarized in Kimura et al. (2003, 2006) provided characteristics of the aggregates that satisfy the observational data for cometary dust. The best fit was achieved

for the monomers of radius 100 nm and the refractive index that was determined based on *in situ* study of comet Halley, which is equal to *1.88+i0.47* for the wavelength λ=450nm and to *1.98+i0.48* for λ=600nm. It appears that for such a dark material a crucial characteristic is the number of monomers in the aggregate. Fig. 5.4 shows that increasing the number of monomers in the aggregate results in a more pronounced negative polarization branch and in a stronger depolarization of the positive polarization. This allows us to suggest that in the case of aggregates of thousands of monomers it is possible to reach the observable values of negative (~0.015) and positive (~0.3) polarization.

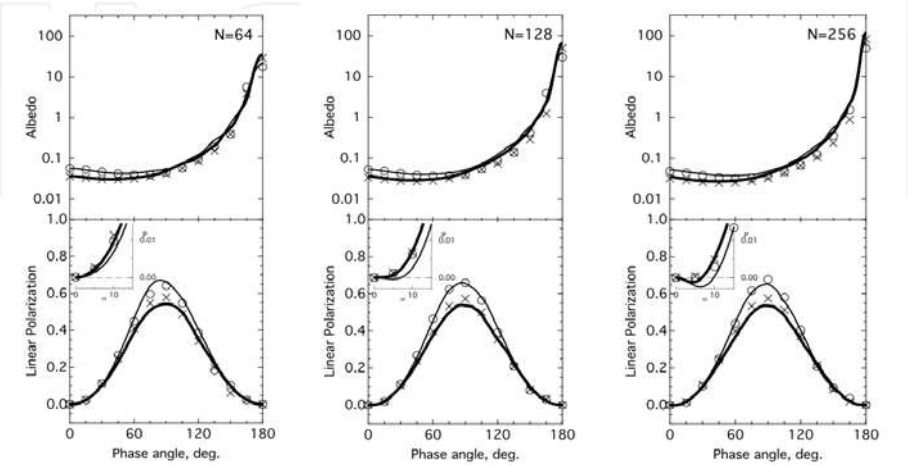

Fig. 5.4. Albedo (in %) and polarization as functions of phase angle depending on the aggregate size (number of monomers in the aggregate). The monomer radius is equal to 100 nm. The refractive index was taken as typical for cometary dust (based on *in situ* data for comet Halley) and is equal to *1.88+i0.47* for the wavelength λ=450nm and *1.98+i0.48* for λ=600nm. The number of monomers in the aggregate is 64 (left panel), 128 (middle panel), 256 (right panel). Development of the negative polarization is shown in the inserts. Notice also a decrease of the polarization maximum more pronounced for the shorter wavelength. The figure was adapted from Mann et al. (2004).

Figs. 5.2-5.4 also demonstrate that the polarimetric color is often less red in the case of more compact BPCAs. We explain this by a stronger depolarization of light in the case of more compact aggregates. Such a depolarization is even more evident from Figs. 3.3 and 4.3 where aggregates with higher packing density (more particles in the volume) always demonstrate smaller polarization maximum. Depolarization of light with increasing packing density is consistent with increasing electromagnetic interaction between the monomers resulted from both diffuse multiple scattering and near-field effects as considered in Sections 3-4

Kolokolova & Kimura (2010) showed that a measure of the depolarization can be the number of monomers covered by a single wavelength; the more monomers the wavelength covers, the more depolarized is the scattered light. It is clear that a single wavelength covers more monomers in the case of more compact aggregates. It also covers more monomers if the wavelength is longer. Thus, we can expect the scattered light to be more

depolarized at longer wavelengths and the color of polarization should be blue. Blue polarimetric color is frequently observed. For example, it is typical for asteroid surfaces and interplanetary dust. However, as we already mentioned, cometary dust has a red polarimetric color. In our opinion, this is good evidence that cometary aggregates are highly porous. For porous aggregates, an increase in the wavelength may not increase the number of monomers covered by a single wavelength. Then the polarimetric color is defined by properties of individual monomers. Specifically, the monomer size parameter decreases with increasing wavelength that moves it closer to the Rayleigh regime of scattering characterized by higher polarization, thus, resulting in the red color of polarization.

An interesting observational result was reported by Kiselev et al. (2008) who summarized the observational data of spectral behavior of comet polarization and showed that cometary dust is characterized by a red polarimetric color in the visible (wavelengths of 400-800nm) but it changes to a blue polarimetric color in the near infrared (wavelengths of 1000-3000nm). They also showed that some comets exhibit a blue polarimetric color even in the visible. These observations can be interpreted based on the dependence of electromagnetic interaction on the number of monomers covered by a single wavelength. Fig. 5.5 illustrates our point. One can see there that in the case of a porous aggregate a small change in the wavelength does not change the number of particles it covers. However, at longer wavelength even in porous aggregates the number of monomers covered by a single

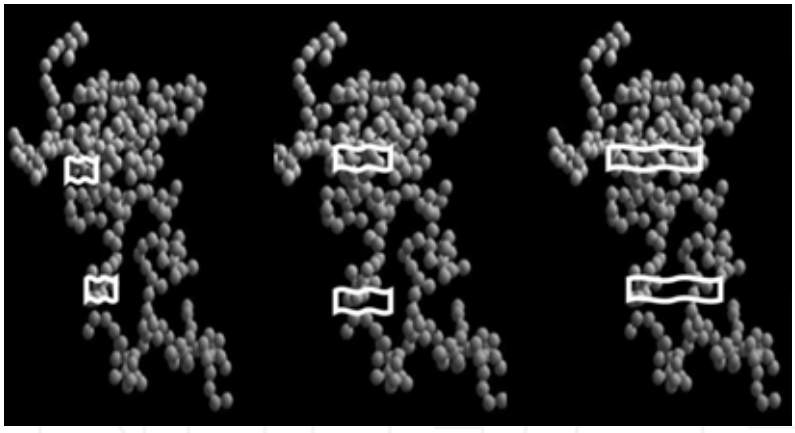

Fig. 5.5. Illustration of the effect of increasing wavelength on the light scattering by an aggregate. In a compact aggregate (top part of the aggregate) the longer the wavelength the more monomers it covers, so the interaction between the monomers becomes stronger, and the light becomes more depolarized. This results in a decrease of polarization with wavelength, i.e. blue color of polarization. For a porous aggregate (bottom part of the aggregate), the number of monomers covered by a single wavelength does not change much as the wavelength increases, i.e. the change in the interaction between the monomers cannot overpower the change in the monomer size parameter, and so the polarization color stays red. However, as the wavelength reaches some critical value, the number of covered monomers in the porous aggregate changes significantly(as shown in the right-hand aggregate) and interaction becomes the main factor that defines the polarization color which then becomes blue.

wavelength increases causing depolarization of the scattered light. This explains the change in the observed polarimetric color as the observations move to the near infrared. In the case of more compact aggregates, even a slight change in wavelength increases the number of covered monomers resulting in blue polarimetric color even in the visible. Thus, it is likely that the dust in the comets with blue polarimetric color, as well as asteroidal and interplanetary dust, is characterized by more compact particles. The wavelength where polarimetric color changes from red to blue may be used to determine the porosity of aggregate particles.

5.2 Spectral manifestation of coherent backscattering

In Section 3.2 we discussed how coherent backscattering affects intensity and polarization phase curves producing there brightness and polarization opposition effects. Recently it has been found that coherent backscattering also manifests itself in spectral data. It affects the depth of the absorption bands and makes it dependent on the phase angle. The physics of this is clear: since coherent backscattering produces brightness opposition effect of different steepness at different absorptions, the steepness of the opposition effect is different within and outside of the absorption bands and, thus, the absorption bands should have different depth and, most likely, shape at different phase angles. This fact was confirmed at observations of Saturn's satellites. Their spectra have distinct ice absorption bands in the near infrared and these bands do change with phase angle (Fig. 5.6). Although this effect has been studied so far for regolith surfaces it should also exist for any medium whose light scattering is affected by coherent backscattering.

We modeled spectral manifestation of the coherent backscattering using the T-matrix code and presenting the surface of Saturn's satellites as a large icy aggregate similar to those described in Sections 3 and shown in Fig. 3.4. Fig 5.7 presents the results of our simulations of the ice absorption band at 2.8 μm at different size of monomers and packing density of the aggregate. One can see that the simulations correctly reproduce the observed tendencies. More so, the variations in the rate of the change of the absorption band depth and shape promise that the study of the spectra at several phase angles can serve as a new remote sensing tool to reveal properties of monomers and their arrangement in aggregates.

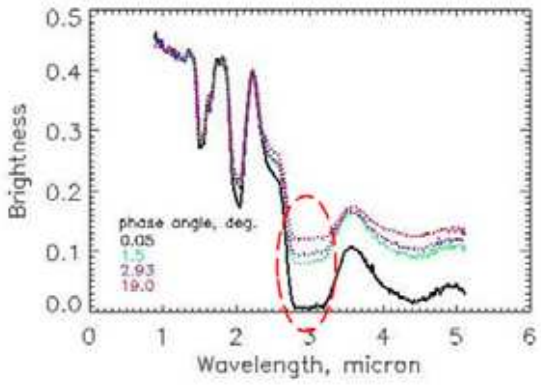

Fig. 5.6. Spectrum of Saturn's icy satellite Rhea at a variety of phase angles (from Kolokolova et al., 2010). It is clearly seen that the depth of the absorption bands varies with phase angle as it should be in accordance with the coherent backscattering. The red dashed ellipse shows the band whose modeling is presented in Fig. 5.7.

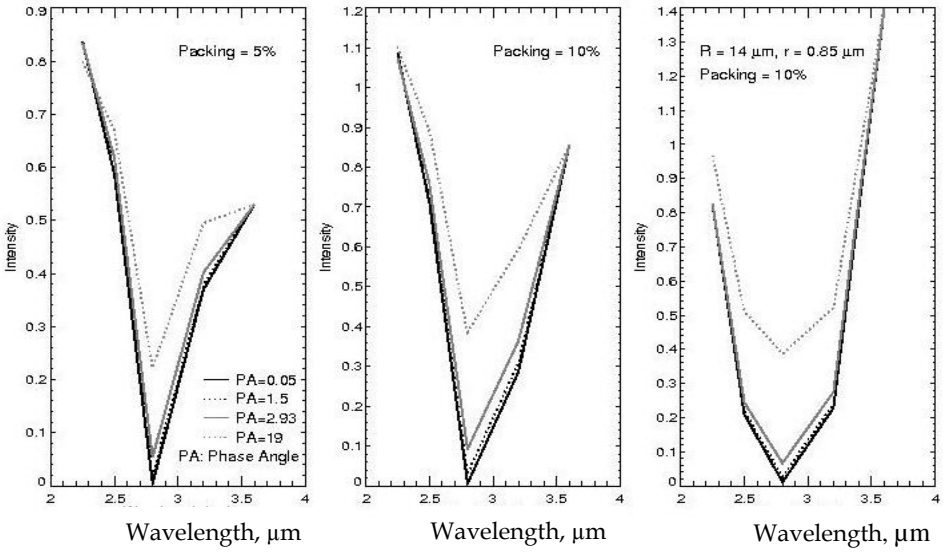

Fig. 5.7. Simulations of the phase angle variations in the spectra of icy aggregates. Different phase angles (PA) are indicated in the left panel. The left panel is for the monomer of radius 1.0 μm and packing 5%, the middle panel is for the same monomers but different packing, 10%, and the right panel is for the same packing as the middle one but for smaller monomers, r= 0.85 μm. In all cases the overall size of the aggregate is 14 μm. Adapted from Kolokolova et al. (2011a).

5.3 Circular polarization of the light scattered by aggregates

Circular polarization was observed in the light scattered by the dust in comets (Rosenbush et al., 2007) and molecular clouds (Hough et al., 2001). It is well known that circular polarization manifests violation of mirror symmetry in the medium. Van de Hulst (1957) showed (see his Section 5.22) that circular polarization arises when the medium has unequal number of left-handed and right-handed identical but mirror asymmetric particles. This immediately shows that if we consider light scattering by a single aggregate, let say BPCA or BCCA, then even in the case of random orientation of this aggregate its circular polarization does not vanish as the majority of ballistic aggregates are asymmetric (Fig. 5.1). This was repeatedly shown by computer simulations of light scattering by aggregates (Kolokolova et al., 2006; Guirado et al., 2007). However, ensembles of natural aggregates, such as cosmic dust, usually do not have domination of particles of a specific handiness. So, in the case when some ensemble of natural aggregates demonstrates circular polarization, it has another violation of mirror symmetry than that resulted from the asymmetric arrangement of the monomers in the aggregates.

One of the most common violations is alignment of elongated particles (e.g., in magnetic field). This is a very common situation for cosmic dust and numerous papers on alignment of aggregates and their circular polarization have been published (see reviews by Lazarian, 2007; 2009 and reference therein). One more opportunity for mirror asymmetry of aggregates is optical activity of their material. Optical activity is typical for organics of

biological origin due to the homochirality of their molecules (i.e. domination of left handed amino acids and right handed sugars). Recently the T-matrix code by Mackowski & Mishchenko (1996) has been updated to allow accounting for the optical activity of the monomer material (Mackowski et al., 2011). Below we show some results of the computer modeling based on this code.

To avoid the influence of mirror asymmetry of the aggregate itself, described above, we performed the calculations for a completely symmetric aggregate like a cube of spheres or 3D-cross. The optical activity was described by a complex parameter $\beta=\beta_r+i\beta_i$ that demonstrated the difference in the complex refractive index for the light with left-handed and right-handed polarization; here βr described the circular birefringence of the material and β_i described its circular dichroism. The code correctly predicted the equal but opposite sign of the circular polarization in the case of aggregates of the opposite sign of β. The modeling by Kolokolova et al. (2011b) showed that the circular polarization quickly increased with increasing optical activity, size of monomers, and especially size of the aggregate. An interesting result was a strong dependence of the circular polarization on the packing density of the aggregates. Fig. 5.8 shows that the circular polarization is much larger and increases more quickly with the size of aggregate in the case when the aggregate is more compact. This probably demonstrates an increasing influence of the diffuse multiple scattering as the aggregate becomes larger or more compact, and more monomers are involved in the light scattering.

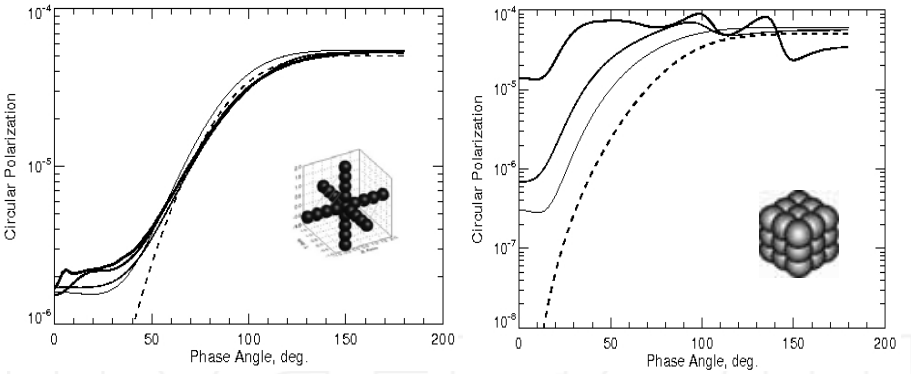

Fig. 5.8. Dependence of absolute values of circular polarization on the size of a 3D-cross aggregate (left) and cubic aggregate (right). The radius of the monomers is 50 nm; the wavelength is 650 nm. The dashed line is for a single monomer; solid lines are for the aggregates of 9, 125, and 343 monomers (thickness of the line increases with the number of monomers). In the simulations we used $m=1.55002+i0.0006002$ *and* $\beta=7.034*10^{-6}-i*0.8692*10^{-8}$ which were estimated based on the measured excess of left-handed amino acids in some meteorites (Pizzarello & Cronin, 2000; Pizzarello & Cooper, 2001).

It is evident that diffuse multiple scattering can affect circular polarization because at each consequent scattering on an optically active monomer circular polarization should increase. This effect is opposite to the depolarization of linearly polarized light in a result of multiple scattering. Linear polarization depends on the plane in which the scattering happens, and at multiple scattering this plane changes randomly thereby randomizing the resultant

polarization (see Section 3.1). Orientation of the scattering plane does not affect circular polarization, and its formation is determined only by the fact that the light repeatedly interacts with optically-active scatterers. Since the cubic aggregate shown in Fig. 5.8 represents the case of a densely packed aggregate, we expect that its light scattering is also affected by near-field effects. How near-field effects influence circular polarization is a topic of a separate study that still needs to be done.

6. Conclusions

We have briefly described a progress recently made in the understanding and modeling of a variety of physical effects associated with electromagnetic interaction between constituent scatterers in a complex object such as an inhomogeneous particle or an aggregate of small monomers. Our test objects were aggregates as a common example of natural particles. In the case when such aggregates are made of particles much smaller than wavelength, effective medium theories can be applied to study their light scattering. However, natural, especially cosmic, particles are aggregates of monomers larger than wavelength when observed in the visible spectral range. Their light scattering requires a more sophisticated approach. We showed that with increasing packing density of aggregates interaction of their monomers becomes more complex and involves diffuse multiple scattering, coherent scattering, and, at even larger packing densities, near-field effects. The diffuse multiple scattering simplifies dependencies of intensity and polarization on phase angle reducing the resonant oscillations typical for single scattering by particles of size larger than wavelength. In its turn, coherent scattering complicates the phase curves adding brightness and polarization opposition feature in the backscattering domain. Development of these features becomes even more complex when the packing density increases and near-field effects become not negligible. The near-field effects affect all phase angles, changing value and location of both the polarization minimum and maximum as well as behavior of the intensity. The correct accounting for all these effects is possible by using rigorous solutions of the Maxwell equations for complex objects. In the case of aggregates, such a solution is provided by the superposition T-matrix approach (Mackowski & Mishchenko, 1996). We use this approach to simulate properties of large aggregates. This allows us not only to study all types of interaction separately and find conditions for their realization, but also to interpret the observational data for cosmic dust. The T-matrix modeling provides: (1) explanation of specifics of phase dependencies of intensity and polarization for cometary and other cosmic dust; (2) explanation of spectral dependence of polarization for comets and asteroids and its variations with wavelength; (3) explanation of variations in depth of spectral bands observed for Saturn's satellites; (4) study of circular polarization of light scattered by objects of biological interest. This modeling also allows us to reveal the characteristics of dust particles in a variety of natural environments thereby validating it as a powerful tool for remote sensing applications.

7. Acknowledgement

This work was supported by a grant of NASA Astrobiology Program and by a grant of Japanese Society for the Promotion of Science.

8. References

Belskaya, I. N., Shkuratov, Yu. G, Efimov, Yu. S., Shakhovskoj, N.M., Gil-Hutton, R., Cellino, A., et al. (2005) The F-type asteroids with small inversion angles of polarization. *Icarus,* 178, pp. 213-221.

Bohren, C., & Huffman, D. (1983) *Absorption and Scattering of Light by Small Particles*, J. Wiley & Sons, NY.

Borghese, F., Denti, P., & Saija, R. (2010) *Scattering from Model Nonspherical Particles: Theory and Applications to Environmental Physics Physics of Earth and Space Environments),* Springer, Berlin.

Bruggeman, D. A. G. (1935) Berechnung verschiedener physikalischer Konstanten von heterogenenSubstanzen. I. Dielektrizitatskonstanten and Leitfahigkeiten der Mischkorper aus isotropen Substanzen. *Annalen der Physik,* 24, pp. 636–664.

Choy, T. C. (1999) *Effective medium theory: principles and applications*, Clarendon Press, Oxford University Press, Oxford England, New York.

Chylek, P, Videen, G., Geldart, D., Dobbie, J., & Tso, H. W. (2000) Effective medium approximations for heterogeneous particles. In: *Light scattering by nonspherical particles* (Mishchenko, M., Hovenier, J., & Travis, L., Eds.), pp. 274-308, Academic Press, NY.

Etemad, S., Thompson, R., Andrejco, W. J., John, S., & MacKintosh, F.C. (1987) Weak localization of photons: termination of coherent random walks by absorption and confined geometry. *Phys. Rev. Lett.,* 59, pp. 1420-1423.

Greenberg, J. M., & Hage, J. I. (1990) From interstellar dust to comets - A unification of observational constraints, *Astrophys. J., Part 1,* 361, pp. 260-274.

Guirado, D., Hovenier, J. W., & Moreno, F. (2007) Circular polarization of light scattered by asymmetrical particles*, J. Quant. Spectr. Radiat. Transfer,* 106, pp. 63-73.

Gustafson, B. Å. S. (1999) Scattering by complex systems I: Methods. In: *Formation and Evolution of Solids in Space (*Greenberg, J. M. & Li, A., Eds.), pp. 535-549, Kluwer Academic Publishers, Dordrecht.

Gustafson, B. Å. S., Greenberg, J. M., Kolokolova, L., et al. (2001) Interactions with Electromagnetic Radiation: Theory and Laboratory Simulations, In: I*nterplanetary Dust,* pp. 509 -523, Springer-Verlag.

Hanner, M. S. (2003) The scattering properties of cometary dust, J. *Quant. Spectrosc. Radiat. Transfer*, 79-80, pp. 164-173

Hanner, M. S., Giese, R. H., Weiss, K., & Zerull, R. (1981) On the definition of albedo and application to irregular particles, *Astron. Astrophys.* 104, pp. 42-46.

Hough, J. H., Bailey, J., Chrysostomou, A., Gledhill, T., Lucas, O., Tamura, M., Clark, S., Yates, J., & Menard, F. (2001) Circular polarization in star-forming regions: possible implications for homochirality, *Advances in Space Research,* 27, pp. 313-322.

Hovenier, J. W., Van der Mee, C., & Domke, H. (2004) *Transfer of polarized light in planetary atmospheres: basic concepts and practical methods,* Kluwer Academic Publishers, Dordrecht.

van de Hulst, H. C., (1957) *Electromagnetic scattering by small particles,* Dover Publ. Inc., New York.

Kimura, H. (2001) Light-scattering properties of fractal aggregates: numerical calculations by superposition technique and the discrete-dipole approximation. *J Quant. Spectrosc. Radiat. Transfer*, 70, 581-594.

Kimura, H., Kolokolova, L., & Mann, I., (2003) Optical properties of cometary dust: Constraints from numerical studies on light scattering by aggregate particles, *Astron.Astrophys.,* 407, L5-L9.

Kimura, H., Kolokolova, L., & Mann, I. (2006) Light scattering by cometary dust numerically simulated with aggregate particles consisting of identical spheres, *Astron.Astrophys.*, 449, pp. 1243 – 1254.

Kiselev, N., Rosenbush, V., Kolokolova, L., & Antonyuk, K. (2008) The anomalous spectral dependence of polarization in comets, *J. Quant. Spectrosc. Radiat. Transfer,* 109, pp. 1384-1389.

Kokhanocsky, A. (2001) *Optics of Light Scattering Media: Problems and Solutions,* Springer, Berlin.

Kolokolova, L., & Gustafson, B. Å. S. (2001) Scattering by inhomogeneous particles: Microwave analog experiment comparison to effective medium theories. *J. Quant. Spectrosc. Radiat. Transfer,* 70, pp. 611-625.

Kolokolova, L., Hanner, M., Levasseur-Regourd, A.-Ch., & Gustafson, B. Å. S. (2004a) Physical properties of cometary dust from light scattering emission, In *Comets II,* (Festou, M. C., Keller, H. U., & Weaver, H. A., Eds.), pp. 577 – 604, Univ.of Arizona Press, Tucson.

Kolokolova, L., Kimura, H., & Mann, I. (2004b) Characterization of dust particles using photopolarimetric data: Example of cometary dust, In: *Photopolarimetry in Remote Sensing* (Videen, G., Yatskiv, Ya., & Mishchenko, M., Eds.), pp. 431 – 454, Kluwer Acad. Publ., Dordrecht-London.

Kolokolova, L., Kimura, H., Ziegler, K., & Mann, I. (2006) Light-scattering properties of random-oriented aggregates: do they represent the properties of an ensemble of aggregates? *J. Quant. Spectr. Radiat. Transfer,* 100, pp. 199-206.

Kolokolova, L., Kimura, H., Kiselev, N., & Rosenbush, V. (2007) Two different evolutionary types of comets proved by polarimetric and infrared properties of their dust. *Astron. Astrophys.*, 463, pp.1189-1196.

Kolokolova, L., Buratti, B., & Tishkovets, V. (2010) Impact of coherent backscattering on the spectra of icy satellites of Saturn the implications of its effects for remote sensing, *Astrophys J. Let.*, 711, L71-L74.

Kolokolova, L., & Kimura, H. (2010) Effects of Electromagnetic Interaction in the Polarization of Light Scattered by Cometary and Other Types of Cosmic Dust, *Astron.Astrophys.*, 513, id.A40.

Kolokolova, L., Liu, L., Buratti, B., & Mishchenko, M.I. (2011a) Modeling variations in the near-infrared spectra produced by the coherent backscattering effect, *J. Quant. Spectrosc. Radiat. Transfer,* DOI: 10.1016/j.jqsrt.2011.03.010.

Kolokolova, L., Sparks, W., & Mackowski, D. (2011b) Astrobiological remote sensing with circular polarization. In: *Polarimetric Detection, Characterization, and Remote Sensing* (Mishchenko, M. I., Yatskiv, Ya. S., Videen, G., & Rosenbush, V. K., Eds.), Springer, Berlin, in press.

Kozasa, T., Blum, J., & Mukai, T. (1992) Optical properties of dust aggregates. I - Wavelength dependence, *Astron. Astrophys.,* 263, pp. 423-432.

Lazarian, A. (2007) Tracing magnetic fields with aligned grains, *J. Quant. Spectr. Radiat. Transfer,* 106, pp. 225-256

Lazarian, A. (2009) Quantitative Theory of Grain Alignment: Probing Grain Environment and Grain Composition, In: *Cosmic Dust - Near and Far (*Henning, Th., Grün, E., & Steinacker, J., Eds.), pp. 482-493, Astromomical Society of the Pacific, San Francisco.

Levasseur-Regourd, A.-Ch., & Hadamcik, E. (2003) Light scattering by irregular dust particles in the solar system: observations and interpretation by laboratory measurements. *J. Quant. Spectrosc. Radiat. Transfer,* 79–80, pp. 903–910.

Li, A., & Greenberg, J. M. (1998) From interstellar dust to comets: infrared emission from comet Hale-Bopp C/1995 O1), *Astrophys.J. Let.,* 498, L83-L87.

Lien, D. J. (1991) Optical properties of cometary dust, In: *Comets in the post-Halley era. Vol. 2* (Newburn R. L., Neugebauer, M., & K. Rahe, Eds.), pp. 1005-1041, Kluwer Acad. Publishers, Dordrecht.

Lumme, K., & Bowell, E. (1981) Radiative transfer in the surfaces of atmosphereless bodies. I. Theory. *Astron. J.* 86, pp. 1694-1704.

Lumme, K., & Rahola, J. (1994) Light scattering by porous dust particle in the discrete-dipole approximation. *Astrophys. J.,* 425, pp. 653-667.

Mackowski, D.W., & Mishchenko, M.I. (1996) Calculation of the T matrix and the scattering matrix for ensembles of spheres. *J. Opt. Soc. Am. A.,* 13, pp. 2266-2278.

Mackowski, D., Kolokolova, L., & Sparks, W. (2011) T-matrix approach to calculating circular polarization of aggregates made of optically active materials, *J. Quant. Spectrosc. Radiat. Transfer,* DOI: 10.1016/j.jqsrt.2011.02.003.

Mann, I., Kimura, H., & Kolokolova, L. (2004) A comprehensive model to describe light scattering properties of cometary dust, *J. Quant. Spectrosc. Radiat. Transfer,* 89, pp. 291-301.

Maxwell Garnett, J. C. (1904) Colours in metal glasses and in metallic films. *Philos Trans Roy Soc A,* 203, pp.385–420.

Meakin, P. (1984) Effects of cluster trajectories on cluster-cluster aggregation: a comparison of linear and Brownian trajectories in two- and three-dimensional simulations. *Phys. Rev. A,* 29, pp. 997–999.

Mishchenko, M. I. (2008) Multiple scattering, radiative transfer, and weak localization in discrete random media: unified microphysical approach. *Rev. Geophys.* 46, RG2003.

Mishchenko, M. I., Hovenier, J.W., & Travis, L.D. Eds.(2000) *Light Scattering by Nonspherical Particles. Theory, Measurements, and Applications.* Academic Press, London.

Mishchenko, M. I., Travis, L. D., & Lacis, A.A. (2002) *Scattering, Absorption, and Emission of Light by Small Particles.* Cambridge Univ. Press, Cambridge.

Mishchenko, M. I., Travis, L.D., & Lacis, A. A. (2006) Multiple scattering of light by particles: Radiative transfer and coherent backscattering. Cambridge Univ. Press, Cambridge.

Mishchenko, M. I., & Liu, L. (2007) Weak localization of electromagnetic waves by densely packed many-particle groups: exact 3D results. *J Quant Spectrosc Radiat Transfer,* 106, pp.616-621.

Mishchenko, M. I., Liu, L., Mackowski, D. W., Cairns, B., & Videen, G. (2007) Multiple scattering by random particulate media: exact 3D results. *Opt. Express,* 15, pp. 2822-2836.

Mishchenko, M. I., Dlugach, J. M., Liu, L., Rosenbush, V. K., Kiselev, N. N., & Shkuratov, Yu. G. (2009a) Direct solutions of the Maxwell equations explain

opposition phenomena observed for high-albedo solar system objects. *Astrophys. J. Let.,* 705, pp. L118-L22.

Mishchenko, M. I., Dlugach, J. M., & Liu, L. (2009b) Azimuthal asymmetry of the coherent backscattering cone: Theoretical results. *Physical Review A*, 80, pp. 053824 – 053832

Mishchenko, M. I., Rosenbush, V. K., Kiselev, N. N., Lupishko, D. F., Tishkovets, V. P., Kaydash, V. G., Belskaya, I. N., Efimov, Yu. S., & Shakhovskoy, N. M. (2010) *Polarimetric Remote Sensing of Solar System Objects*, Akademperiodyka, Kyiv.

Muinonen, K. (1990) *Light scattering by inhomogeneous media: backward enhancement and reversal of linear polarization.* PhD dissertation, University of Helsinki, Finland.

Mukai, T. (1989) Cometary dust and interplanetary particles. In: *Evolution of Interstellar Dust and Related Topics* (Bonetti, A., Greenberg J. M., & Aiello, S., Eds.), pp. 397-445, North-Holland, Amsterdam.

Mukai, T., Ishimoto, H., Kozasa, T., Blum, J., & Greenberg, J. M. (1992) Radiation pressure forces of fluffy porous grains, *Astron. Astrophys.,* 262, pp. 315-320.

Okada, Y., & Kokhanovsky, A. A. (2009) Light scattering and absorption by densely packed groups of spherical particles. *J Quant Spectrosc Radiat Transfer,* 110, pp. 902-917.

Petrova, E. V., Jockers, K., & Kiselev, N. N. (2000) Light Scattering by Aggregates with Sizes Comparable to the Wavelength: An Application to Cometary Dust. *Icarus*, 148, pp. 526-536.

Petrova, E. V., Tishkovets, V. P., & Jockers, K. (2004) Polarization of light scattered by Solar system bodies and the aggregate model of dust particles. *Solar System Res.*, 38, pp. 309-324.

Petrova, E. V., Tishkovets, V. P., & Jockers, K. (2007) Modeling of opposition effects with ensembles of clusters: Interplay of various scattering mechanisms, *Icarus,* 188, pp. 233-245.

Petrova, E. V., Tishkovets, V. P., & Jockers, K. (2009) Interaction of particles in the near field and opposition effects in regolith-like surfaces, *Sol. System Res.,* 43, pp. 100-115.

Petrova, E.V., & Tishkovets, V.P. (2011) Light scattering by aggregates of varying porosity and the opposition phenomena observed in the low-albedo particulate media. *J Quant Spectrosc Radiat Transfer*, DOI: 10.1016/j.jqsrt.2011.01.011.

Pizzarello, S., & Cronin, G. R. (2000) Non-racemic amino acids in the Murray and Murchison meteorites, *Geochimica et Cosmochimica Acta*, 64, pp. 329-338.

Pizzarello, S., & Cooper, G. (2001) Molecular and chiral analyses of some protein amino acid derivatives in the Murchison and Murray meteorite, *Meteoritics & Planetary Science*, 36, pp. 897-909.

Rosenbush, V., Kiselev, N., Avramchuk, V., & Mishchenko, M. (2002) Photometric and polarimetric opposition phenomena exhibited by Solar system bodies. In: *Optics of Cosmic Dust* (Videen, G., & Kocifaj, M., Eds.) pp. 191-224 Kluwer Academic Publishers, Dordrecht.

Rosenbush, V., Kolokolova, L., Lazarian, A., Shakhovskoy, N., & Kiselev, N. (2007) Circular polarization in comets: Observations of Comet C/1999 S4 LINEAR) and tentative interpretation, *Icarus,* 186, pp. 317-330.

Schuerman, D. W. (1980) *Light scattering by irregularly shaped particles.* New York, Plenum Press.

Shen, Y., Draine, B. T., & Johnson, E. T. (2008) Modeling Porous Dust Grains with Ballistic Aggregates. I. Geometry and Optical Properties, *Astrophys. J.*, 689, pp. 260-275.

Shkuratov, Yu. G. (1989) New mechanism of the negative polarization of light scattered by atmosphereless cosmic bodies. *Astron Vestnik,* 23, pp. 176–180 [in Russian].

Shkuratov, Yu. G., Muinonen, K., Bowell, E., Lumme, K., Peltoniemi, J. I., Kreslavsky, V.F., Stankevich, D.G., Tishkovetz, V.P., Opanasenko, N.V., & Melkumova, L.Y. (1994) A critical review of theoretical models of negatively polarized light scattered by atmosphereless Solar system bodies. *Earth, Moon, & Planets*, 65, pp. 210-246.

Shkuratov, Yu., Ovcharenko, A., Zubko, E., Miloslavskaya, O., Muinonen. K,. Piironen, J., et al. (2002) The opposition effect and negative polarization of structural analog for planetary regoliths. *Icarus*, 159, pp. 396-416.

Shkuratov, Yu., Ovcharenko, A., Zubko, E., Volten, H., Munoz, O., & Videen, G. (2004) The negative polarization of light scattered from particulate surfaces and of independently scattering particles. *J. Quant. Spectrosc. Rad. Transfer,* 88, pp. 267-284.

Shkuratov, Yu. G., & Grynko, Ye. S. (2005) Light scattering by media composed of semitransparent particles of different shapes in ray optics approximation: consequences for spectroscopy, photometry, and polarimetry of planetary regoliths. *Icarus*, 173, pp.16-28.

Sihvola, A., (1999) *Electromagnetic Mixing Formulae and Applications,* IEE Publ., London.

Tishkovets, V. P. (1998) Backscattering of light by close-packed system of particles. *Opt. Spectrosc.,* 85, pp. 212–217.

Tishkovets, V. P., Shkuratov, Yu. G., & Litvinov, P. V. (1999) Comparison of collective effects at scattering by randomly oriented cluster of spherical particles. *J. Quant. Spectrosc. Radiat. Transfer,* 61, pp. 767–773.

Tishkovets, V., Litvinov, P., Petrova, E., Jockers, K., & Mishchenko, M. (2004a) Backscattering effects for discrete random media. In:. *Photopolarimetry in remote sensing* (Videen, G., Yatskiv, Ya. S., & Mishchenko, M. I., Eds), pp. 221-242, Kluwer Acad. Publ., Dordrecht.

Tishkovets, V. P., Petrova, E. V., & Jockers, K. (2004b) Optical properties of aggregate particles comparable in size to the wavelength, *J. Quant. Spectrosc. Radiat. Transfer*, 86, pp. 241-265.

Tishkovets, V. P. (2008) Light scattering by closely packed clusters: shielding of particles by each other in the near field. *J Quant Spectrosc Radiat Transfer,* 109, pp. 2665-2672.

Voshchinnikov, N. V. (2004) *Optics of cosmic dust,* Cambridge, UK: Cambridge Scientific Publishers.

Voshchinnikov, N. V., Il'in, V. B., & Henning, Th. (2005) Modelling the optical properties of composite and porous interstellar grains, *Astron. Astrophys.*, 429, pp.371-381

Voshchinnikov, N. V., Il'in, V. B., Henning, Th., & Dubkova, D. N. (2006) Dust extinction and absorption: the challenge of porous grains, *Astron. Astrophys.*, 445, pp.167-177.

Voshchinnikov, N., V., Videen, G., & Henning, Th. (2007) Effective medium theories for irregular fluffy structures: aggregation of small particles, *Applied Optics IP,* 46, pp.4065-4072.

West, R. A. (1991) Optical properties of aggregate particles whose outer diameter is comparable to the wavelength. *Appl. Opt.,* 30, pp. 5316–5324.

Wolff, J., Clayton, G. C., & Gibson, S. J. (1998) Modeling composite and fluffy grains. II. Porosity and phase function. *Astrophys. J.*, 503, pp. 815–830.

Zubko, E., Shkuratov, Yu., Mishchenko, M., & Videen, G. (2008) Light scattering in a finite multi-particle system. *J Quant Spectrosc Radiat Transfer,* 109, pp. 2195–2206.

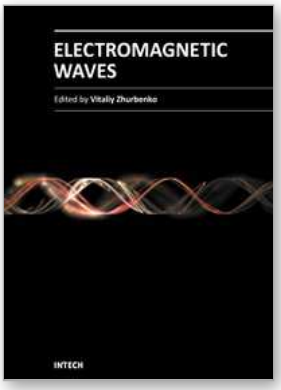

Electromagnetic Waves
Edited by Prof. Vitaliy Zhurbenko

ISBN 978-953-307-304-0
Hard cover, 510 pages
Publisher InTech
Published online 21, June, 2011
Published in print edition June, 2011

This book is dedicated to various aspects of electromagnetic wave theory and its applications in science and technology. The covered topics include the fundamental physics of electromagnetic waves, theory of electromagnetic wave propagation and scattering, methods of computational analysis, material characterization, electromagnetic properties of plasma, analysis and applications of periodic structures and waveguide components, and finally, the biological effects and medical applications of electromagnetic fields.

InTech Europe
University Campus STeP Ri
Slavka Krautzeka 83/A
51000 Rijeka, Croatia
Phone: +385 (51) 770 447
Fax: +385 (51) 686 166
www.intechopen.com

InTech China
Unit 405, Office Block, Hotel Equatorial Shanghai
No.65, Yan An Road (West), Shanghai, 200040, China
中国上海市延安西路65号上海国际贵都大饭店办公楼405单元
Phone: +86-21-62489820
Fax: +86-21-62489821